Selectivity and Mechanism in Catalytic Asymmetric Synthesis*

John M. Brown
Dyson Perrins Laboratory, University of Oxford, South Parks Road, Oxford OX1 3QY

1 Background to Homogeneous Catalysis

A catalyst can affect both the reactivity and selectivity of organic transformations, and affords the possibility of conducting organic synthesis in a highly controlled manner. Yet there are only two types of catalysts which have been widely applied for this purpose, namely enzymes (either isolated or as cell or organism preparations) and homogenous transition-metal complex catalysts. The physicochemical understanding of enzyme mechanism goes back almost a century,[1] but the appreciation of organometallic catalysis has a much more recent vintage.[2] Before any involvement in the details of homogeneous catalysis is attempted, it may be useful to compare the attributes of the two types. As Figure 1 indicates, there are fundamental differences between the way in which enzymes catalyse organic reactions and the way in which organometallic catalysis is effected.

The complexity, and hence the available information content of an enzyme with an RMM in excess of 10 000 Daltons is much greater than that of the organometallic catalyst of RMM 300—1000 Daltons. This permits the high degree of evolutionary fine tuning in enzyme structure, with two particular consequences – the substrate is matched to the enzyme active site by both steric (repulsive) and electrostatic (attractive) forces, and its recognition by the enzyme is a global effect in that groups remote from the active site can affect specificity and reactivity.[3] With organometallics, steric effects are dominant and the recognition process tends to be limited to the region of the reactive site. A further feature is that reactions can proceed rapidly through intermediates with a strong covalent M–C bond. This means that metal-bound ligands can exert a powerful influence on the bound substrate. Consider the platinum aryl of Figure 2 which is a model for biaryl cross-coupling.[4] The proximity of P-aryl groups to the *o*-anisyl residue enforces restricted rotation about the Pt–C bonds so that there are three atropisomeric forms of the complex, corresponding to the possible Pt-aryl orientations. The *X*-ray structure of the major form with the most relevant fragment dissected demonstrates why this is so.

The type of catalytic reaction relevant to this lecture comes within the ambit of *reductive homogeneous catalysis* whereby a complex in low-valent state activates hydrogen or a related species for transfer to an organic reactant. The best known catalyst in this class is due to Wilkinson, and the likely mechanism of olefin hydrogenation[5] incorporates all the main reaction types encountered in catalysis. A *cis*-biphosphine rhodium chloride fragment remains unchanged throughout the catalytic cycle shown in Figure 3. This in turn activates H_2, associates with the olefin, transfers hydride to the coordinated double bond, and eliminates the alkyl and hydride fragments to revert to the starting complex. The addition and alkene association steps take place respectively to 14e and 16e coordinatively unsaturated complexes – a critical feature of the catalysis. Note that none of the intermediates have been characterized in solution, and the stereochemistry is still a matter for debate.[6] The *cis*-relationship of the two PPh_3 ligands is based on the experimental observation of low catalytic activity in related complexes with *trans*-constrained chelating diphosphines and models which indicate a high degree of steric clashing between catalyst and *Z*-disubstituted olefins in a *trans*-ligand disposition.

Enzyme catalysis	*Organometallic catalysis*
Electrostatic match between substrate and active site an important part of the recognition process.	Discrimination on the basis of steric effects - selective repulsion.
Major factor is desolvation of reactants by transfer from H_2O to the active site.	Moderately strong covalent binding in complexation.
Sensitivity to the overall shape and molecular structure of the reactant.	Reactive site recognition - insensitive to the overall molecular structure (lower dimensionality).
Transition-state often of different geometry to the bound reactant resting state.	Ligand–metal structure similar in resting state and transition state.

Figure 1 Comparison between the salient features of enzymic and organometallic catalysis.

The homogenous hydrogenation of prochiral alkenes can give rise to enantiomerically enriched products. This brings the first, and in many ways the most spectacular success of catalytic asymmetric synthesis into play. The basic reaction involves the hydrogenation of a dehydroamino acid or related structure with diphosphine rhodium complex, and many variants on both catalyst and reactant have been described. Much of the impetus in synthesizing chiral diphosphines comes from this area, and the basic types of effective ligand are shown – as their cationic Rh complexes – in Figure 4.

Although there might be expected to be strong similarities between hydrogenation with Wilkinson's catalyst and these asymmetric reactions, there are important distinctions as well. The reaction mechanism has been defined through careful kinetics carried out by Halpern and co-workers[6] and through the delineation of reactive intermediates in solution through NMR techniques by ourselves.[7] Most work has been carried out with the P-chiral ligand DIPAMP used in the commercial asymmetric synthesis of L-DOPA by Monsanto over many years. The scheme presented in Figure 5 reveals the key features

John Brown graduated from Manchester University and carried out his Ph.D. there with A. J. Birch. After itinerant postdoctorals in New York (Breslow), Canberra, and Bristol (Whiting) he went as a Lecturer in Chemistry to the then new University of Warwick and stayed there until 1974. He moved to the Dyson Perrins Laboratory and Wadham College as Lecturer and Tutor in Organic Chemistry and has remained there since, insulated (in the view of some colleagues elsewhere) from the harsh realities of the real world. His research interests lie in a mechanism-based approach to the understanding and development of chemical catalysis.

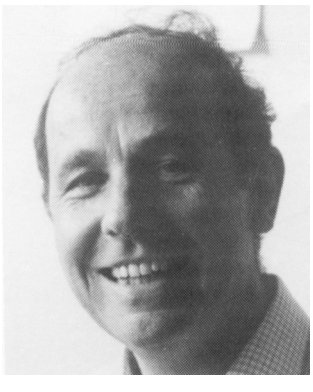

* Based on the Royal Society of Chemistry Tilden Lecture given by the author, 1991.

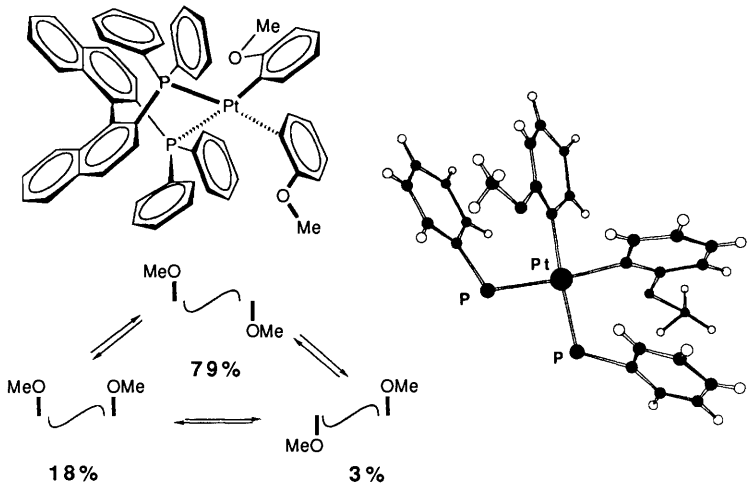

Figure 2 Conformational locking in a chiral platinum alkyl (Jésus Perez-Torrente, Nat Alcock).

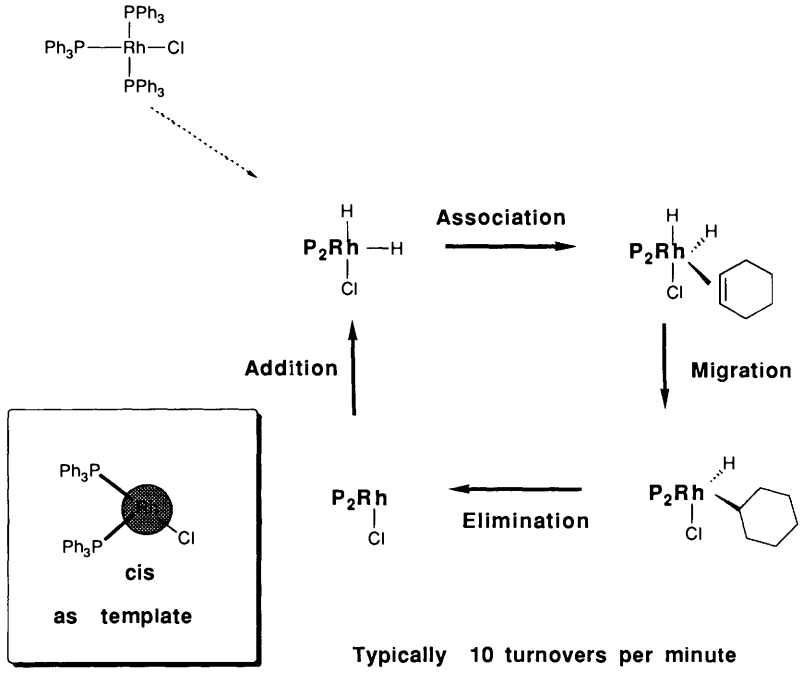

Figure 3 The basic steps in organometallic catalysis, exemplified by the mechanism of hydrogenation with Wilkinson's catalyst.

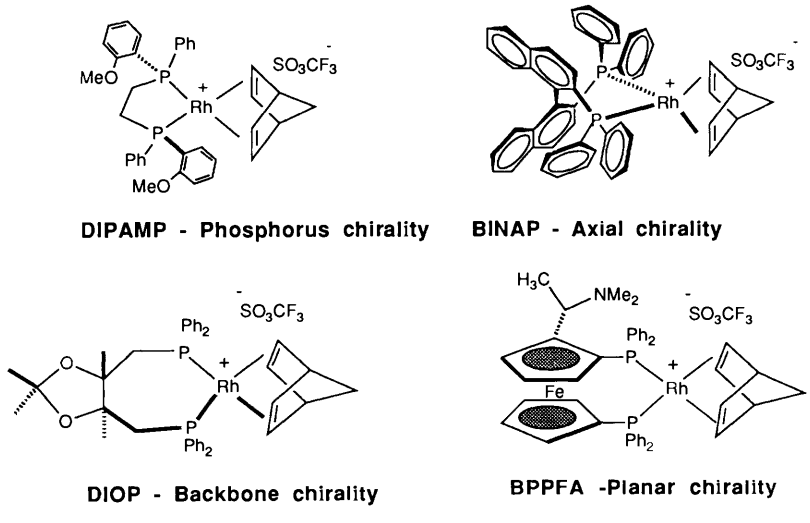

Figure 4 Types of chiral diphosphine ligand.

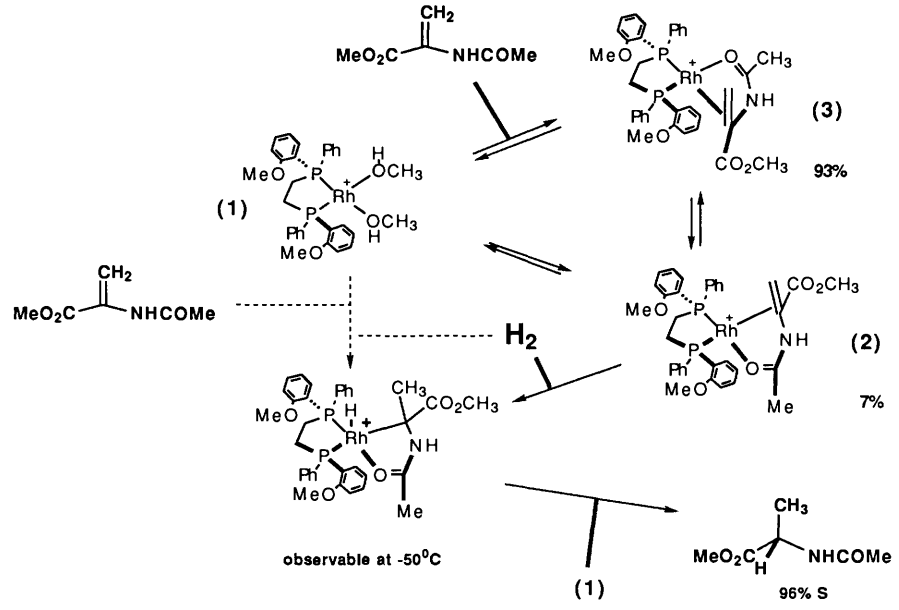

Figure 5 Possible pathways involved in the asymmetric hydrogenation of enamides

of the reaction, there are two diastereomeric enamide complexes in rapid equilibrium on the timescale of H_2 addition and the less favoured of these is configurationally related to an alkylrhodium hydride which can be characterized at low temperatures without the intervention of an observable dihydride [8] The lack of ortho–para hydrogen interconversion indicates that the addition step is irreversible, in contrast to the case of Wilkinson's catalyst Further information on the chemistry of alkyl hydrides comes from studies on their more stable iridium analogues [9]

The uniqueness of dehydroamino acid reactants becomes apparent on consideration of this mechanism At all stages in the cycle where the reactant is rhodium-bound, the amide is coordinated Thus a tight chelate is formed involving the olefin and the amide, locating the reactant precisely within the coordination sphere In the accepted mechanism the two diastereomeric enamide complexes are in equilibrium with the solvate and compete for H_2 addition, with the less stable the more reactive so that it dominates the catalytic turnover The higher reactivity of the minor diastereomer can be predicted by molecular modelling, albeit at a rather crude level [10] There are several *X*-ray studies of coordinated enamides[11] and the fragmented view of Figure 6 demonstrates the substrate environment in that intermediate, complex **A** the more stable and therefore less reactive diastereomer It is noteworthy that nearly all the selectivity arises from steric interactions in one sector of the complex for the major diastereomer involving the carboxylate group (an ethyl ester in this case) and one of the four P-aryl residues The atoms involved in van der Waals contact are starred The minor diastereomer is similar but critical atoms are significantly closer and in addition the vinylic C–H is close to an adjacent P-aryl residue In the hydrogen addition step, steric interactions in the major diastereomer **A** increase dramatically as the complex shifts towards octahedral coordination For the minor diastereomer **B** (adapted from the *X*-ray coordinates of **A**) in which the relative disposition of side-chain and ligand is different, this process occurs without substantial steric opposition

A central feature in rhodium asymmetric hydrogenation is this apparent higher reactivity of the minor enamide complex, which is a general rule irrespective of the ligand structure From a more formal standpoint, the experimental observations point to a reversal of configuration at the stereogenic centre α-to the amide between the favoured diastereomer of the bound enamide and the reduction product Because the interconversion of enamide diastereomers is fast compared to H_2 addition, these observations do not formally require a reaction of hydrogen directly with the bound substrate complex, but it is the simplest explanation consistent with the known facts One has, however, to take alternatives seriously In this, the solvate present at low concentration reacts with hydrogen to form an η^2-complex

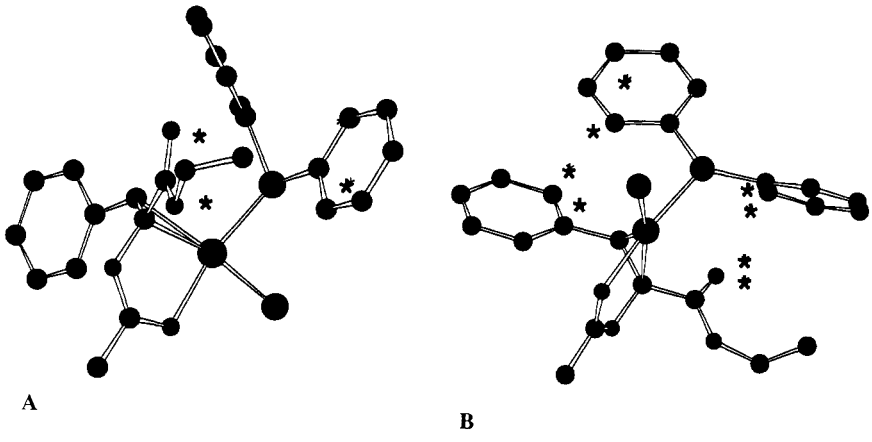

Figure 6 Thermodynamically favoured (**A**, unreactive stereoisomer) and disfavoured (**B**, reactive isomer) in the asymmetric hydrogenation of enamides

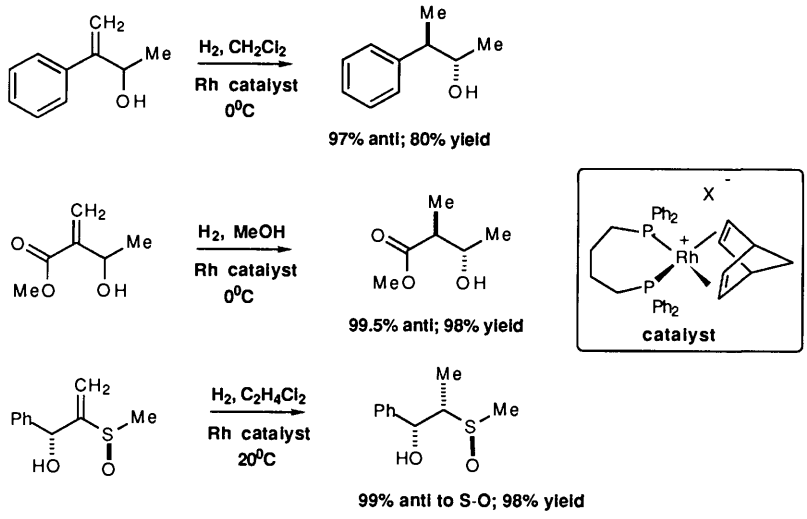

Figure 7 Examples of directed hydrogenation in acyclic systems.

reversibly. Its trapping by substrate is irreversible and occurs in the rate-limiting step. This alternative is kinetically equivalent, but violates the principle of Occam's razor; it is simpler to conceive of observable intermediates rather than transients sustaining the catalytic cycle. In this case the arguments relating to the origin of stereoselection are similar, since the enamide becomes bound to a rhodium which already has H_2 in place so that a 5/6-coordinate species is formed with different constraints to the observed square planar species.

The next section demonstrates how similar principles can be applied in other areas of catalytic hydrogenation. The stereoselectivity described above is derived from *catalyst control*, and we shall now examine the possible consequences of *substrate control*, by incorporating the relevant stereogenic centre in the reactant rather than the catalyst.

2 The Mechanism of Directed Hydrogenation

Rhodium asymmetric hydrogenation is based on the availability of a metal-binding group in proximity to the alkene; there is a transfer of chirality from the ligand to the prochiral centre undergoing hydrogen addition. If the metal-binding group is associated with a stereogenic centre, then a diastereoselective process can occur through intramolecular chirality transfer. This process may be effected with an achiral catalyst/ligand combination, and a simple example[12] developed at the beginning of the project is shown in Figure 7; coordination of the hydroxyl group to rhodium provides the stereochemical control leading to predominance of the *anti*-diastereomer over the *syn*-diastereomer by 97:3. Later work demonstrated that an electron-withdrawing group at the α-position of the olefin provided higher reactivity and stereoselectivity (normally > 99% *anti*), and that other metal-binding groups could be deployed in place of hydroxyl, notably CO_2R, NHCOR, or SOR.[13] It is possible to provide a hierarchy of directing groups, and the results of Figure 8 demonstrate that in direct competition the 5-ring chelate formed from an allylic ester overrides the more basic amide (6-ring chelate) or hydroxyl (4-ring chelate) functions.[14] It is also evident that the sulphoxide group can exert a powerful directing effect even against competition from −OH.[13]

If an asymmetric catalyst is used for the reaction, the diastereoselective hydrogenation is accompanied by kinetic resolution

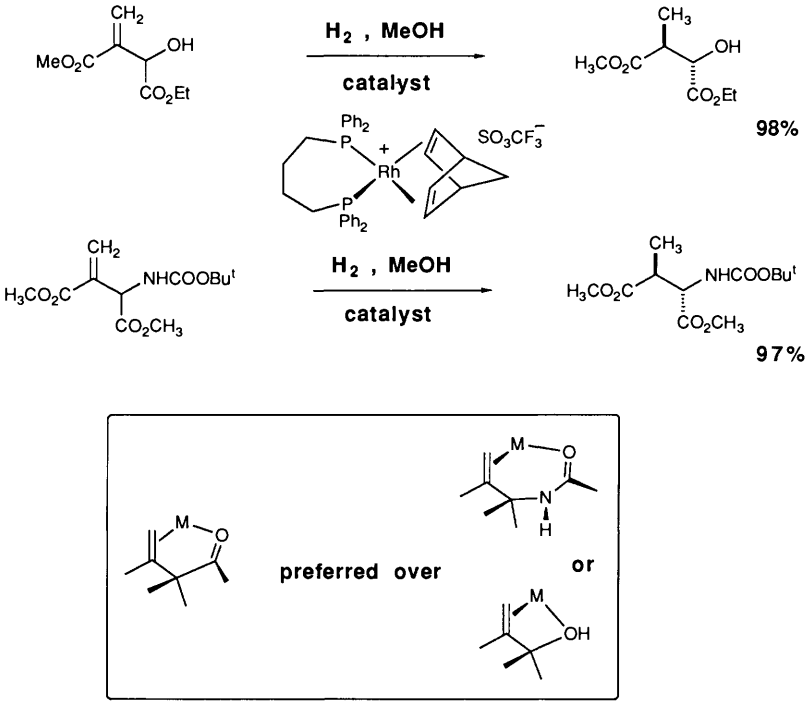

Figure 8 Competition between directing groups in hydrogenation (David Hulmes, Frances Knight).

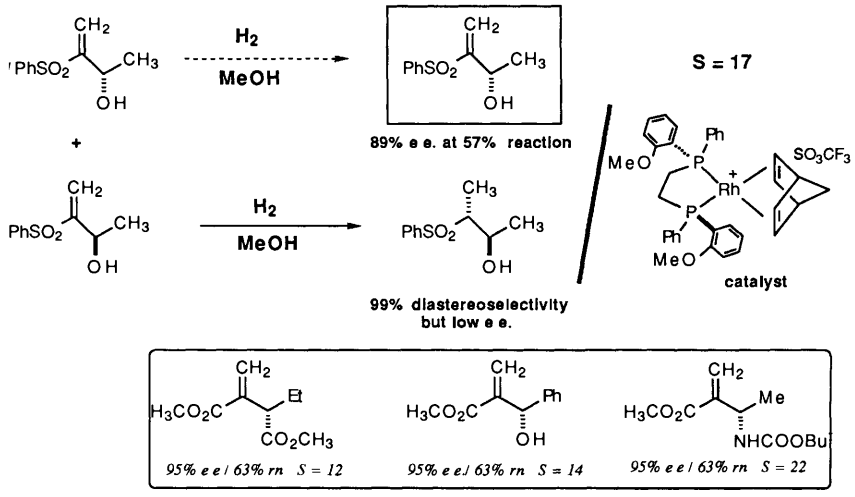

Figure 9 Kinetic resolution of vinylsulfones (David Price)

of the racemic reactant [15] Examples are shown in Figure 9 The selectivity in favour of the fast-reacting enantiomer is in the range of 8 1 to 23 1 depending on the structure of the reactant and the precise reaction conditions, when DIPAMP is the ligand then the configuration of the product is what would be predicted on the basis of enamide hydrogenations This level of efficiency implies that the reactant can be recovered in 95% e e at around 63% (± 4%) reaction Since many of the racemic reactants are very simply prepared in bulk, this affords a simple route to enantiomerically pure acrylates and related compounds

Two distinct stereoselective processes occur in directed hydrogenation with an asymmetric catalyst The diastereoselectivity is a result of *substrate control*, meaning that the existing stereogenic centre in the reactant is responsible for defining the relative configuration at the new centre produced in the reduction The enantioselectivity is a result of *catalyst control*, and can be broadly understood in terms of the earlier discussions on asymmetric hydrogenation, since the reactant structures are similar in the context of the common acrylic acid fragment, and the important role of the carboxylate side-chain Separate analysis of these two features should lead to a complete understanding of both directed hydrogenation and the attendant kinetic resolution

It was recognized from the outset that the reason for *anti*-selectivity in directed hydrogenation was tied in with chelation of the reactant to rhodium, and reduced internal non-bonded interactions between the carboxylate residue and the chiral centre, compared with comparable intermediates on the *syn*-selective pathway The reaction may be seen in the context of addition reactions of α-chiral olefins, the subject of a lively discussion over several years with most emphasis on allylic alcohols and ethers [16] For present purposes, and with some risk of over-simplification, reactions of this type may be divided into two classes, those which proceed through open transition-states typified by hydroboration, and those which proceed through metal-chelated transition-states typified by directed hydrogenation (Figure 10) Broadly speaking, the two categories proceed with opposite diastereoselectivity The hydroboration reaction has been studied in some depth both theoretically and experimentally, and the main conclusion is that reaction proceeds through a sterically preferred ground-state conformation with the allylic C–H eclipsing the double-bond (torsion angle C=C···C–H = 0°) For directed hydrogenation, a consideration of the constraints imposed by chelation indicates that the preferred torsion angle C=C···C–H will be 180°, to minimize the van der Waals interaction between the alkyl group at the chiral centre and the olefin α-substituent Note that this explanation does not depend on the structure of the catalyst, and applies

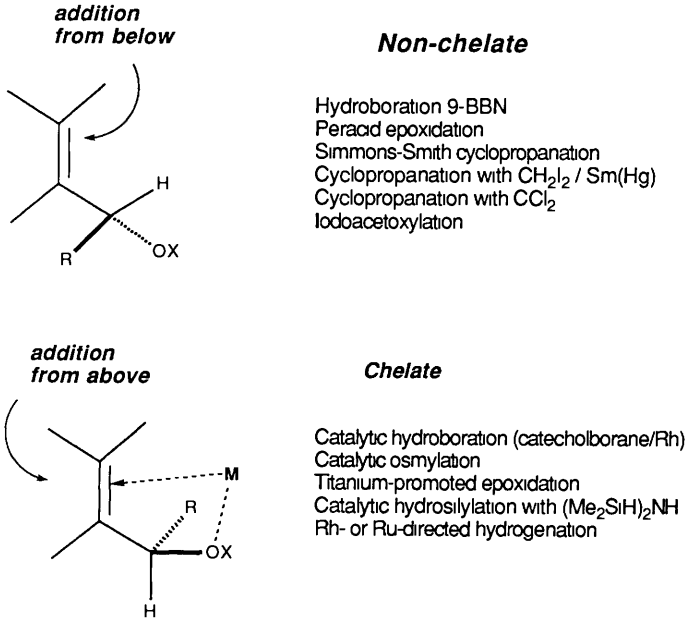

Figure 10 Acyclic stereoselection comparison between chelate and non-chelate models

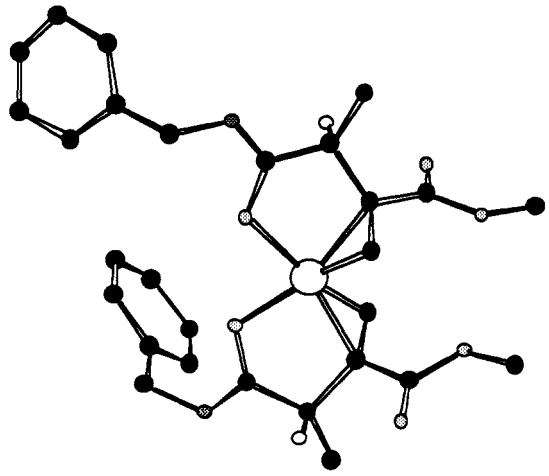

X-Ray structure of the cationic complex formed from $ClIr(C_2H_4)_4$ and

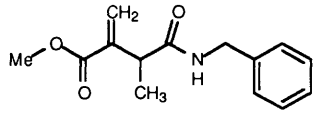

Figure 11 The *X*-ray structure of an iridium complex as a model for the stereochemical course of directed hydrogenation (Alun James, Nat Alcock).

to any step in the catalytic cycle where the double bond and directing group are both coordinated. It suggests that the structure of the reactant rather than the product or an alkylmetal precursor is the dominant factor.

Evidence to underpin this hypothesis comes from the *X*-ray crystal structure of a related iridium complex. In previous work we had shown that dehydroamino esters form stable iridium bischelate cationic complexes.[17] Reaction of the substituted itaconamide ester shown in Figure 11 with $ClIr(C_2H_4)_4$, and anion exchange, gave a single racemic diastereomer of product (of sixteen possible racemates) in high yield.[18] This has the relative configuration of the amide chiral centre and coordinated olefin suggested by directed hydrogenation results; the relevant torsion angle C=C···C=C−H is 5° for one of the ligands and 3° for the other. This structure provides the only close model for the stereochemical course of directed hydrogenation.

Further support for the preferred form of a bound chelate complex is derived from molecular mechanics. Calculations have been carried out for several of the reactants using MMX parameterization to determine the energy of (a) the ground-state conformation, (b) the torsionally constrained structure corresponding to the chelate leading to the *anti*-product, and (c) the related structure leading to the *syn*-product. In Figure 12 the results of these calculations are shown for the simple hydroxyacrylate, and clearly demonstrate a disfavouring of the *syn*-pathway due to the increased steric compression in the bound reactant. This is the case for all other directed hydrogenation reactants subjected to analysis in this way, the correct stereochemical course is predicted on the basis of non-bonded interactions in the reactant without reference to the ligand metal combination of the catalyst.

In addition, a detailed analysis of the kinetics of directed hydrogenation has been carried out.[18] Since the reactants are rather similar in structure to the familiar dehydroamino acids of asymmetric hydrogenation, it seemed logical to study the reaction using a chiral catalyst. One of the main features of enamide hydrogenation is that the prochiral olefin forms two diastereomeric olefin complexes which are in rapid equilibrium *via* both intramolecular and intermolecular paths (Section 1). With a chiral racemic olefin and an enantiomerically pure catalyst, each hand of the reactant can give rise to two distinct complexes corresponding to the *syn* and *anti* routes. Discounting the disfavoured *syn*-pathway, the two complexes of *anti*-disposition are bound through opposite faces of the olefin and correspond to the major and minor enamide complexes in dehydroamino acid reduction. There is however an important distinction: the enamide complexes interconvert, but the chiral olefin complexes are derived from distinct molecules, as indicated in Figure 13. This permits the separate study of pure enantiomers of the reactant and comparison of their reactivity with that of the racemic mixture.

Preparatory work was carried out with racemic dimethyl 3-methylitaconate, which could be satisfactorily resolved by partial hydrogenation with the RhBINAP complex as shown in Figure 14. The enantiomeric purity of the products derived by respectively using the *R*- and *S*-hands of catalyst was determined using the ^{31}P NMR method recently reported by Parker and Taylor.[20] By this means it was demonstrated that the samples were respectively 97%(*R*) and 98%(*S*) enantiomerically pure. Their separate hydrogenation was carried out using *R,R*-Rh DIPAMP to reveal an interesting double asymmetric induction – for the slow-reacting *R*-enantiomer, the diastereomeric purity of *R,R*-dimethyl 2,3-dimethylsuccinate was around 99%. In contrast, the diastereomeric purity of the *S,S*-dimethyl 2,3-dimethylsuccinate derived from the fast-reacting *S*-enantiomer was 99.95%, pushing GC analysis to its limit.

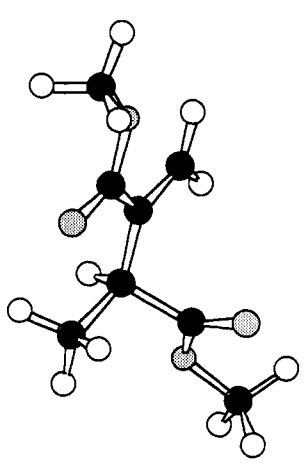

Disfavoured form

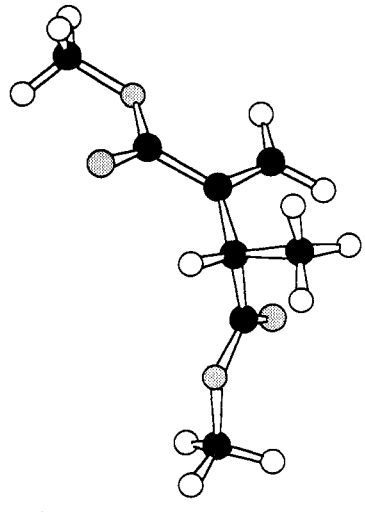

Favoured form (-2 5 kcals/mole)

Figure 12 Molecular mechanics (MMX) derived energy minima for dimethyl 3-methylitaconate in [LHS] disfavoured binding orientation and [RHS] favoured binding orientation.

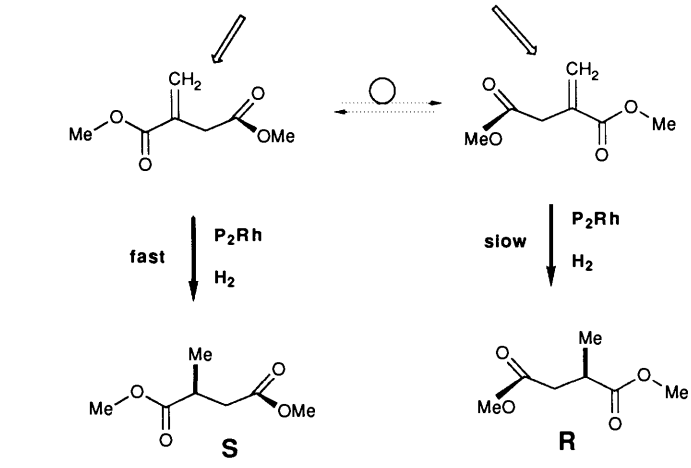

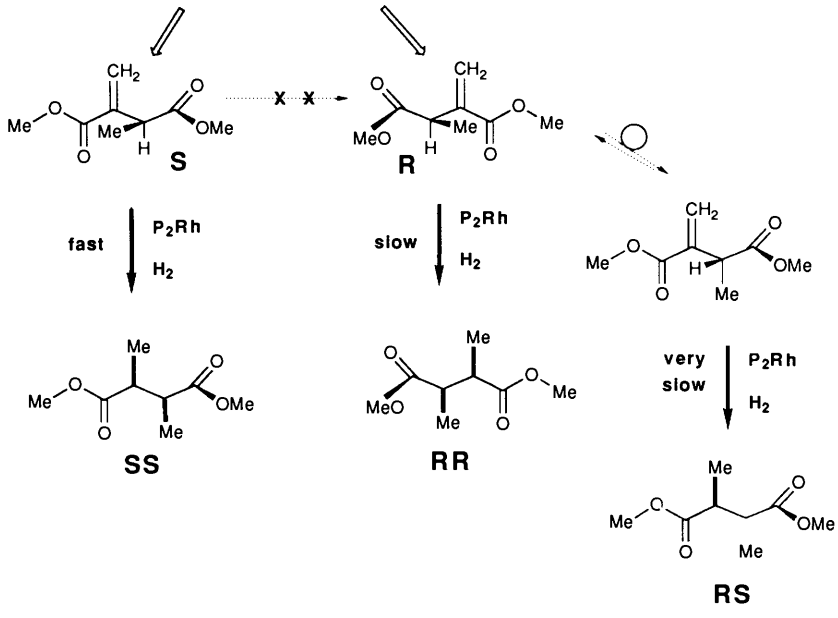

Figure 13 Schematic comparison of the protocols of asymmetric hydrogenation of a prochiral reactant and kinetic resolution of a racemic chiral reactant

Quantitative studies of hydrogenation are difficult If carried out at constant pressure, then some levelling device has to be incorporated to compensate for the absorption of gas during the reaction It is also necessary to enclose the apparatus in a constant-temperature environment In addition, it is conventionally the case that the solution remains saturated with H_2, so that transport across the gas – liquid interface must be very fast in relation to uptake These difficulties were largely circumvented by carrying out hydrogenation in the constant volume apparatus shown in Figure 15 which was used for some of the experiments described here, and which is suitable for studies between 500 and 1700 mbar This is suitably calibrated for diffusion rates across the gas–liquid interface, for the vapour pressure of solvent, and for total enclosed volume During the course of reaction the pressure diminishes, and this causes a voltage signal to be transmitted to the attached microcomputer *via* a pressure transducer A data file of pressure *vs* time is recorded and stored Since the pressure varies with time, and gas diffusion is important for the faster reactions studied, an analytical solution was not attempted Rather, simulation of the data against an experimental model was carried out using the GEAR kinetics program [21] This model is shown in Figure 16, based on the kinetic analysis of enamide hydrogenation and assuming that rate-determining H_2 addition occurs to a bound substrate rather than to the solvate complex [*An alternative kinetically equivalent path has never been seriously discussed because it requires reversible reaction of the Rh solvate with hydrogen to form an* η^2*-dihydrogen complex followed by its irreversible reaction with the substrate and the species involved are unprecedented*] The separate reduction *R*- and *S*-enantiomers of substrate with the RhDIPAMP catalyst is displayed in Figure 17, representing a series of runs carried out at 0 °C, the analysis of these and related reductions according to the model of Figure 16 is inset The key feature emerges immediately, in that the *R*-enantiomer reacts around 40 times faster than the *S*-enantiomer, after correcting for catalyst concentration, and although this is reflected in vastly different rates of reaction with hydrogen it is the slow-reacting enantiomer which binds more strongly This conclusion is reinforced by a ^{31}P NMR study in which it was shown that only the *S*-enantiomer formed a definable complex on reaction with the methanol solvate from RhDIPAMP, starting either from pure enantiomer or from the racemate

The simplest interpretation of kinetic resolution in directed hydrogenation is that the two enantiomers of reactant compete freely for the catalyst, and the two diastereomeric complexes thus formed compete freely for hydrogen This is implicit in the

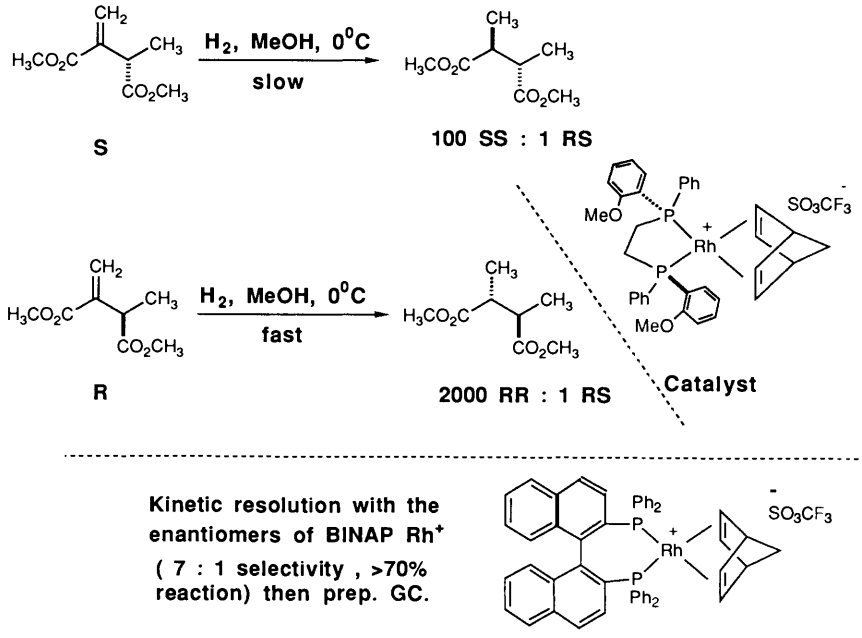

Figure 14 Double asymmetric induction in the hydrogenation of enantiomers of dimethyl 3-methylitaconate.

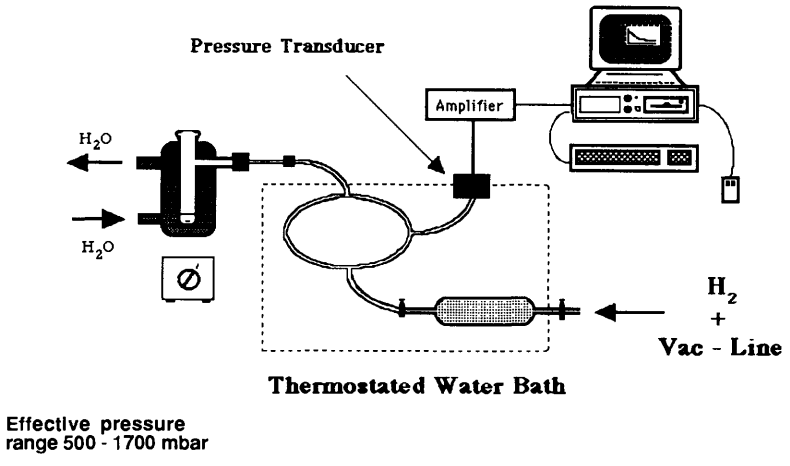

Figure 15 Constant volume hydrogenation apparatus (Alistair Conn, David Price).

G	$\underset{k_{-1}}{\overset{k_1}{\rightleftharpoons}}$	H	Gas-phase/solution interfacial equilibrium
C + S	$\underset{k_{-2}}{\overset{k_2}{\rightleftharpoons}}$	B	Equilibrium between bound solvent and substrate
B + H	$\xrightarrow{k_3}$	C + P	Rate-determining irreversible addition of hydrogen

Figure 16 Kinetic model for directed hydrogenation/kinetic resolution.

model used for the kinetics of reaction of the pure enantiomers. If this is so, then the parameters employed in Figure 17 could be used to give an accurate simulation of the reduction of the racemate with RhDIPAMP as catalyst. This is indeed the case, as the data displayed in Figure 18 indicate. Allowing for a small amount of pre-reaction largely confined to the fast enantiomer the agreement between experiment and theory is well within experimental error. This does not of course prove the proposed mechanism (since the alternative suggested earlier would have the same kinetic form) but it does show that it is consistent with the observed kinetics. Experiments which formally distinguished between the two pathways (H_2 addition to the Rh solvate followed by substrate trapping being the alternative to the generally accepted H_2 addition to the bound substrate complex) would be highly desirable.

3 The Mechanism of Asymmetric Transfer Hydrogenation

Conventionally, hydrogenations are carried out in a two-phase system with gaseous hydrogen and a rapidly stirred solution in contact. Several methods are known in which the reduction is effected with concomitant oxidation of a reagent, which can be a dihydroaromatic compound, a secondary alcohol, or formic acid. The first successful example of asymmetric hydrogenation using this technique is due to Brunner and Leitner,[22] and mechanistic studies have been carried out at Oxford in collaboration with the same group. The basic reaction is shown in Figure 19; for convenience, the HCO_2H/NEt_3 azeotrope is utilised and DMSO is found to be the most effective solvent. The ratio of reductant to substrate is 1:1 and there is an isotope effect associated with the C–H(D) of formic acid. Several pathways can be envisaged, among them (a) the Rh-catalysed decomposition of formate to give H_2 *in situ* which is subsequently scavenged by Rh and reacts *via* conventional catalytic hydroge-

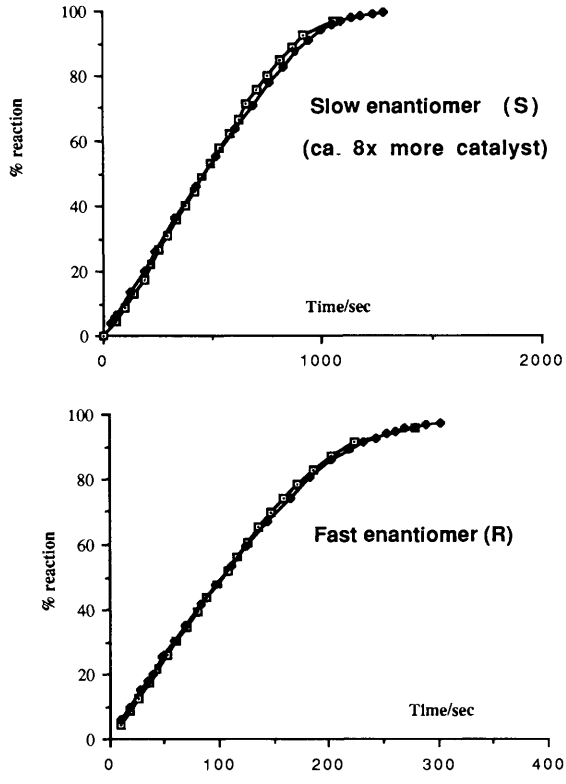

Simulation of kinetic runs with pure enantiomers

For the slow-reacting (S)-enantiomer binding constant K (k_2/k_{-2})= 240 mol l^{-1} and rate constant k_3 = 8.1 mol l^{-1} s^{-1}

For the fast-reacting (R)-enantiomer binding constant K (k_2/k_{-2})= 52 mol l^{-1} and rate constant k_3 = 420 mol l^{-1} s^{-1}

Figure 17 Results with pure enantiomers of dimethyl 3-methylitaconate; □, experimental points; ◆, predictions of model (Alistair Conn).

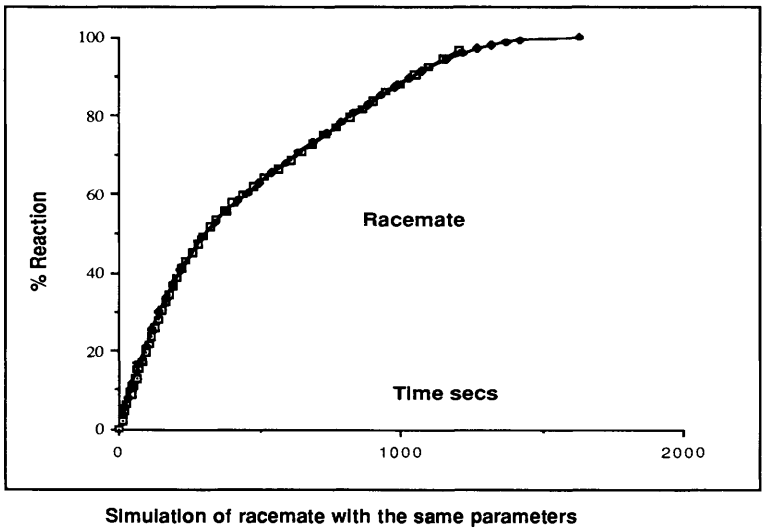

Figure 18 Results with racemic dimethyl 3-methylitaconate; □, experimental points; ◆, predictions of model (Alistair Conn).

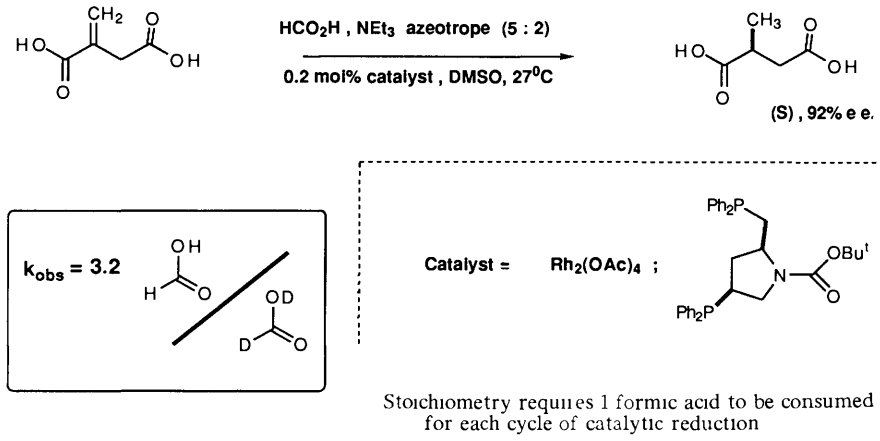

Figure 19 Background to asymmetric transfer hydrogenation

nation, (b) the activation of HCO_2H so that the proton is transferred first in the coordination sphere to substrate, followed by collapse of the alkylformate complex to alkylhydride, and (c) the activation of HCO_2H to give CO_2 and a metal dihydride which subsequently traps and reduces the olefin

Homogeneous hydrogenation is known to be a stereospecific *syn*-addition [23] In order to test whether this is the case for transfer hydrogenation, reaction of the doubly prochiral E-phenylitaconic acid was examined using dideuterated formic acid The product was a single diastereoisomer by ^1H NMR, identical to that obtained in the hydrogenation of the same reactant with deuterium (Figure 20) This leads to the conclusion that the two deuterium atoms in transfer hydrogenation are transferred with *syn*-specificity, making the link to the conventional reaction pathway

One attractive feature is that the two hydrogens transferred to the olefin are formally distinct and their distribution in the product may give insights into the two separate stages of hydride transfer This indicated a useful set of experiments based on monodeuterated formates, which were again carried out with *E*-phenylitaconic acid Since the formic acid proton is in rapid exchange with carboxylic acids it was necessary to ensure that all the acidic protons in a given experiment were in either O–H or O–D form Interestingly, the reaction of this substrate is rather slower than that of the parent itaconic acid, and there is no appreciable isotope effect with DCO_2H as reductant Even so, the formate decomposition is irreversible and less than 5% protium has been incorporated in residual DCO_2H at 100% reduction

The results obtained are shown in Figure 21 and are rather surprising They appear to indicate that the H and D sites in formic acid become scrambled during the catalytic cycle and cannot be distinguished in the product This suggests that a rhodium dihydride must be formed and the two Rh-H sites become equivalent before any transfer to the olefin occurs But there is a competing process which part-scrambles the hydrogens intermolecularly, perhaps through reversible dimerization, this then explains the formation of d_0 and d_2-isotopomers starting either from HCO_2D or DCO_2H, even at short reaction times A simple method of analysing the product was devised employing $\{^1H\}\{^2H\}^{13}C$ NMR spectroscopy (Figure 22) Under these decoupling conditions each isotopomer of product appears as a single line – isotopic shifts are additive in ^{13}C NMR spectroscopy[24] – and concurrent analysis of the data from the several sites permits accurate results

Further work was carried out employing kinetic resolution to probe the mechanism This necessitated the synthesis of both pure enantiomers of 3-methylitaconic acid, carried out as in Section 2 with subsequent acid hydrolysis of the diester Since the enantioselectivity in itaconic acid reduction is around 90%, the two hands of 3-methylitaconic acid would be expected to show an approximate 20 1 rate ratio to express the same enantiofacial selectivity In practice they react at rates within a factor of two of one another Assuming that they are like the parent itaconic acid in reactivity (*i e* with HCO_2H involved in the rate-limiting step, and a primary kinetic isotope effect) then it implies that binding of the substrate imparts very little control This is in contrast to observations made for the related hydrogenation reaction where (with RhDIPAMP as catalyst) the *R*- and *S*-enantiomers react at substantially different rates Kinetic resolution of the racemate was also carried out, analysing the product at 53% and 70% reaction with HCO_2H and RhBPPM catalyst (Figure 23) Here the recovered reactant is substantially resolved, employing ^{31}P NMR analysis of the Pt(DIOP) complexes as before to determine the e e The selectivity factor S is 16 for these experiments, in accord with expectation from asymmetric hydrogenation of the parent

How then do we accommodate a selectivity which is evident for kinetic resolution of the racemate, but which is not revealed in the relative reactivity of the two hands of reactant reduced separately? The most consistent explanation is that the rate-determining decomposition of formate occurs with little influence by the reactant, which may bind reversibly at that stage It is only after the bound formate has decomposed that the role of the substrate becomes important, the results are consistent with the mechanism outlined in Figure 24, which is closer to the 'alternative' pathway discussed in Section 2 than to the accepted route [24] Obviously new experiments will have to be devised if it is to be demonstrated that this mechanism has any bearing on conventional Rh asymmetric hydrogenation

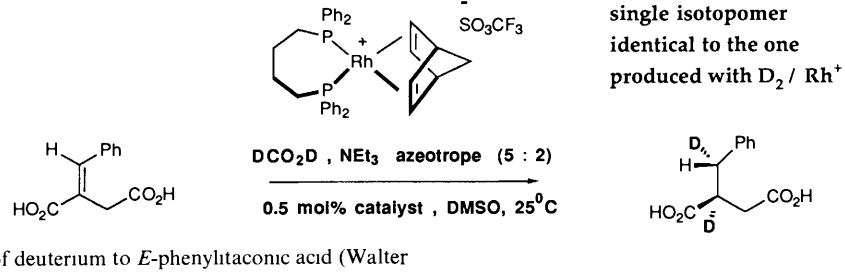

Figure 20 *syn*-Addition of deuterium to *E*-phenylitaconic acid (Walter Leitner)

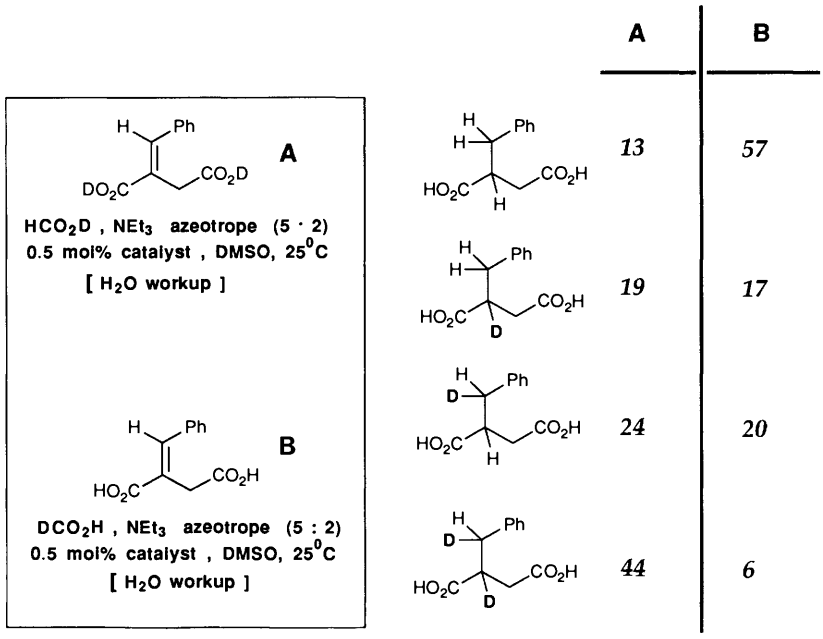

Figure 21 Regiochemistry in the addition of H–D *via* transfer hydrogenation (Walter Leitner)

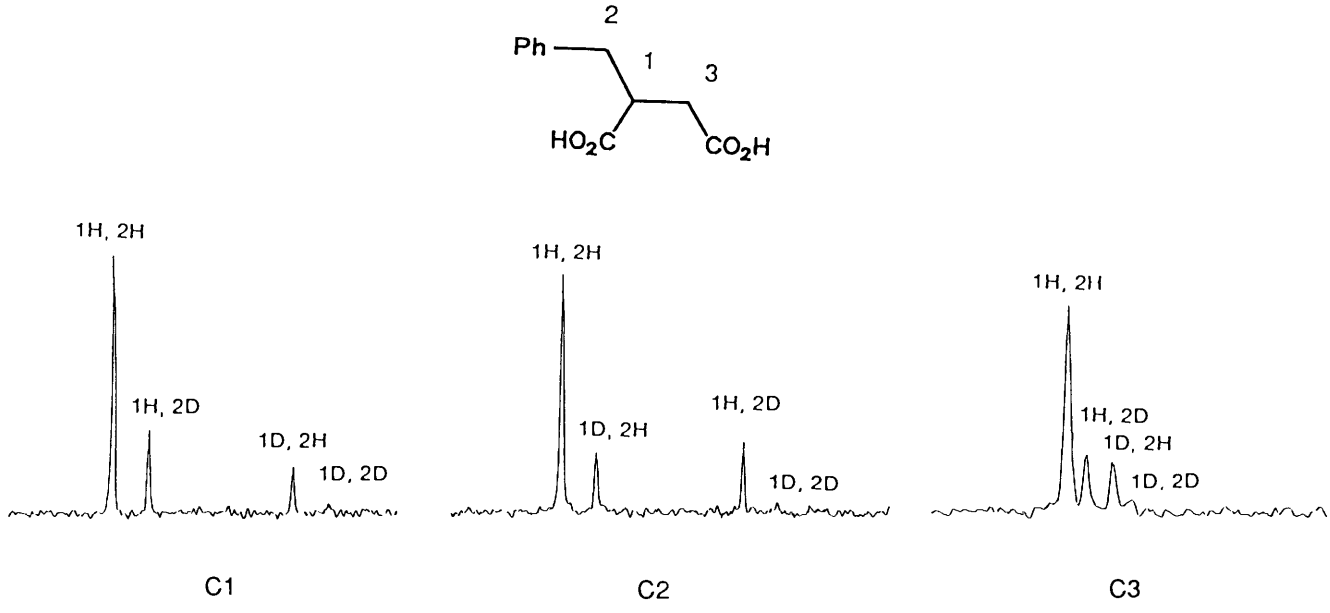

Figure 22 Deuterium-decoupled ^{13}C NMR of the reaction product from H D addition in transfer hydrogenation (Walter Leitner)

4 Extensions of Ruthenium Asymmetric Hydrogenation

The most striking set of results in asymmetric hydrogenation in the last five years has been concerned with ruthenium rather than rhodium chemistry [25] The RuBINAP catalyst, associated most closely with Noyori, has been spectacularly successful for reduction of a wide range of functional olefins and ketones with uniformly high enantioselectivity That is not to say that the methodology is perfect however, in many cases the reactivity of the olefin is low, and considerable fine-tuning may be required in the case of any given reactant to achieve the desired enantioselectivity This means that there is room for development of new strategies The catalyst syntheses[26] used tend to be rather specific for BINAP It is desirable to have catalysts which are less rigid and thus potentially more reactive, and achieve specificity through a greater degree of pre-organization We first sought a general route to Ru^{II} diphosphine complexes and then tried to understand their chemistry by comparison with rhodium catalysis

The route finally adopted is shown in Figure 25, and is based on early Ru^{II} chemistry developed by Schrock, Lewis, and Johnson [27] In this route the diolefin is displaced in the final step by the desired ligand to give a stable species exemplified by the ferrocenylbiphosphine complex shown, which is crystallographically characterized [28] When BINAP was utilised as the ligand there was ^{31}P NMR evidence for two complexes corresponding to the λ and δ forms at the ruthenium metal centre, in common with other chiral diphosphines All diphosphines tried gave rise to characterizable complexes of the desired structure

It was initially found that the complexes were not hydrogenation catalysts, although they were reactive towards formic acid in the presence of a substrate and therefore effective transfer hydrogenation catalysts,[29] although in cases other than the itaconic acid reduction shown in Figure 26 the e e s were moderate The reaction conditions, involving refluxing THF, were very simple to effect

Conventional hydrogenation reactions were carried out after it was discovered that the Ru complexes could readily be

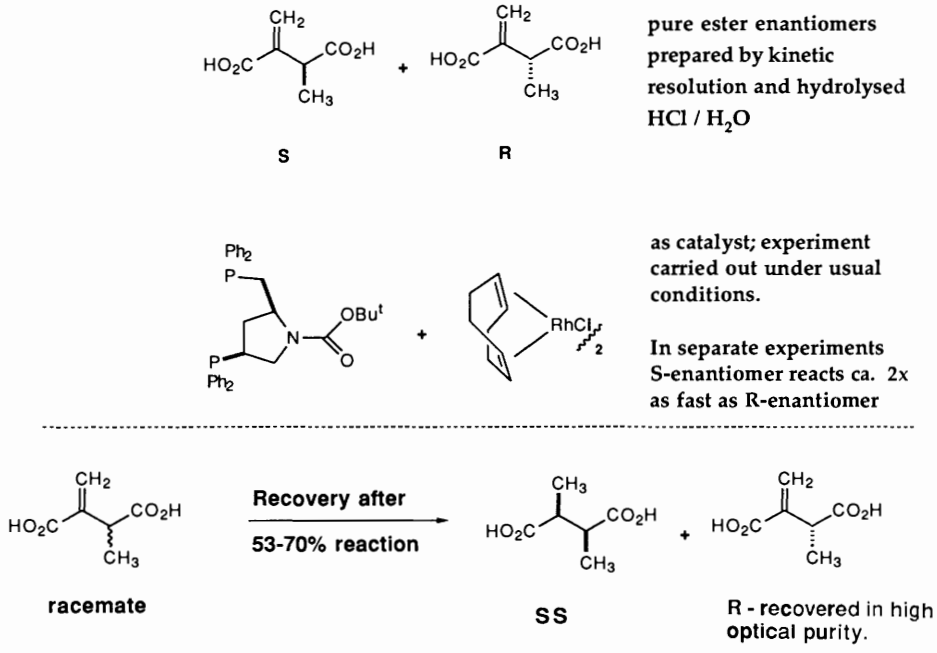

Figure 23 The kinetic resolution experiment applied to transfer hydrogenation (Walter Leitner).

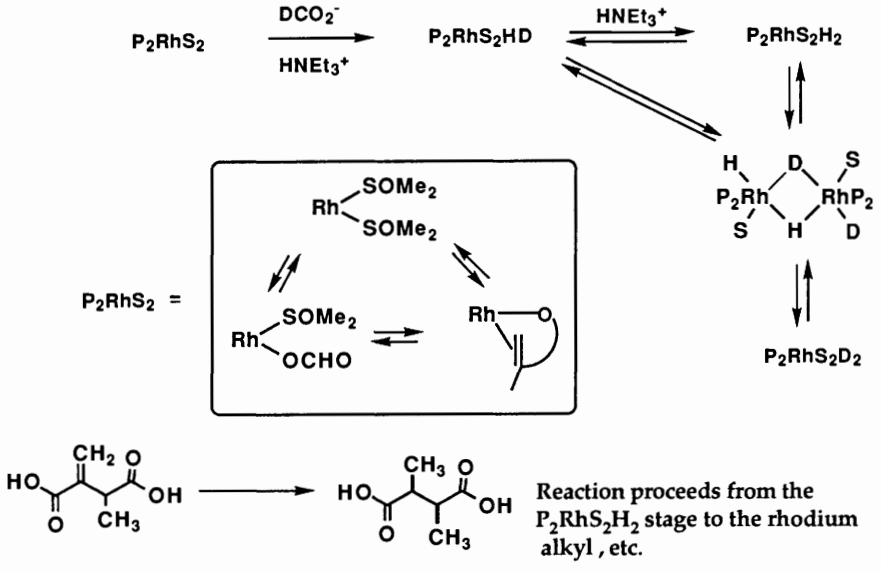

Figure 24 A mechanism consistent with the experimental observations for asymmetric transfer hydrogenation (Walter Leitner).

activated with $Me_3SiOSO_2CF_3$. The structure of the intermediate formed is not yet known, but the acac and f_6-acac complexes are different in reactivity in catalytic hydrogenation (the former a more effective catalyst) leading to the likelihood that it is the η^3-allyl residue which is lost in the activation process, possibly to be replaced by a labile covalent triflate ligand. The ^{31}P NMR of the intermediate shows that the species has become very dynamic and only gives a sharp AB quartet characteristic of two bound phosphorus nuclei in different environments at $-40\,^{\circ}C$. Whilst this structure is speculative the underlying chemistry provides a means of carrying out catalytic hydrogenation with any diphosphine ruthenium catalyst. The first contributions have already been made to the mechanism of RuBINAP hydrogenations,[30] with one particularly interesting feature. Ashby and Halpern report the hydrogenation of unsaturated carboxylic acids and show that the rate law is of the form:

$$k_{(obs)} = 2k[Ru]_{tot}[H_2]/\Sigma\{[S] + [P]\}$$

where [S] and [P] represent the concentrations of reactant and product respectively

consistent with a competition between reactant and product for the active species. Rapid turnovers were achieved under ambient conditions at very low concentrations of catalyst ($\leqslant 10^{-4}$M). If the reduction was carried out with D_2 in MeOH, then only one deuterium was incorporated α to the carboxylate; the β-site incorporates protium from the solvent. Parallel work from the Japanese group also reports a range of deuteration results which corroborate these findings, although under preparative conditions the reactions required more forcing conditions; the American authors comment that hydrogenations are more reproducible in quartz than in Pyrex although the latter may be

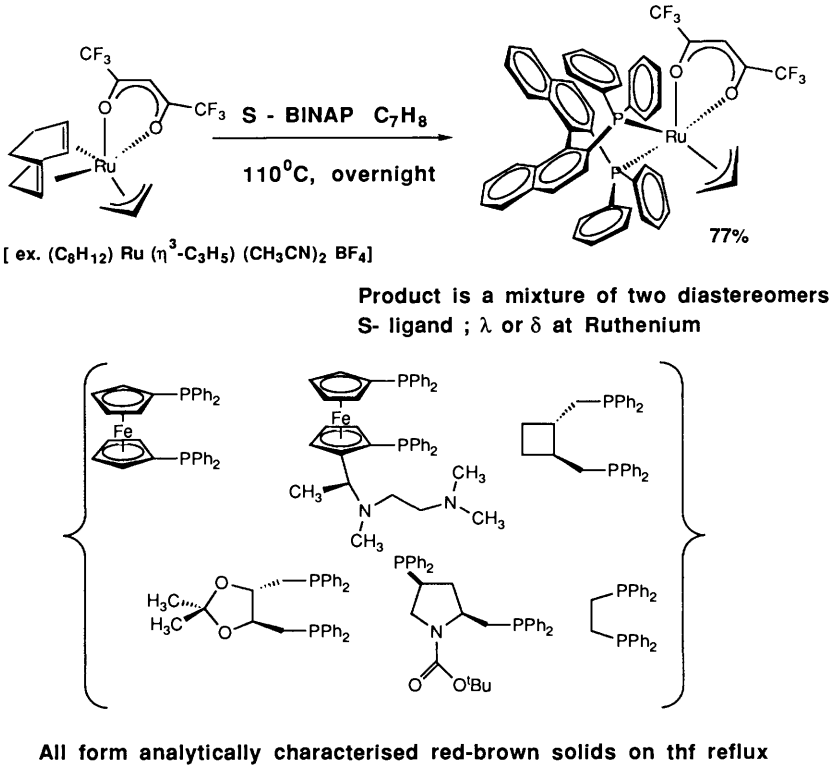

Figure 25 The synthesis of diphosphine ruthenium complexes for catalysis (Michael Rose).

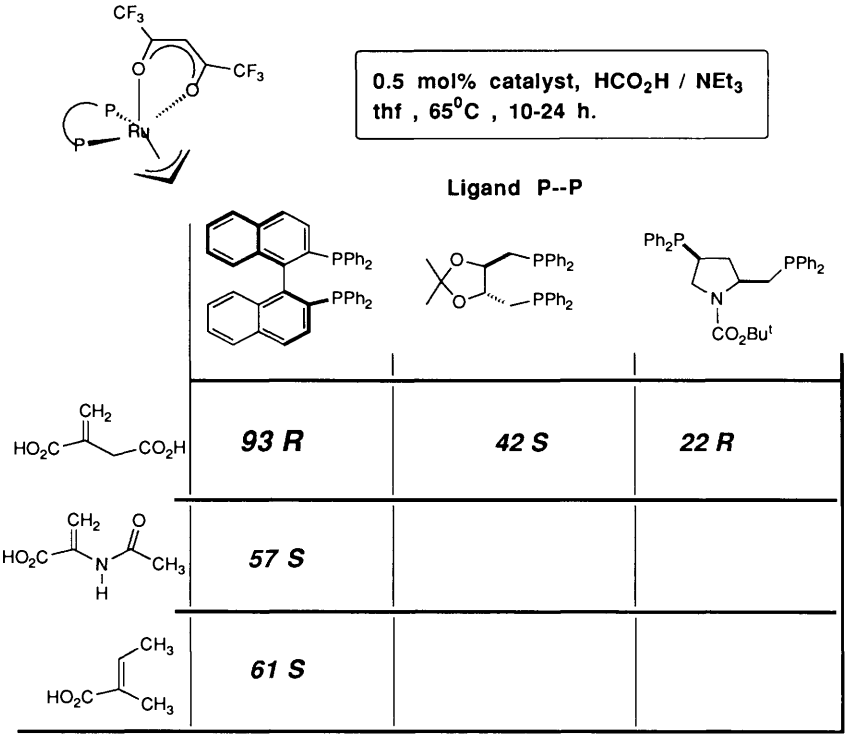

Figure 26 Transfer hydrogenation with the ruthenium complexes (Walter Leitner, Michael Rose).

suitably conditioned by silanization. Whilst there are exchange mechanisms which can account for the observations, Ashby and Halpern suggest that the isotope distribution is a consequence of a formally heterogeneous hydrogenation (Figure 27) in which a hydride ion is first transferred to the catalyst–substrate complex, with protonation of the solvent, and then the resulting chelate alkylruthenium complex is transformed into product by proton transfer to ruthenium, followed by RH elimination.

The availability of achiral complexes described above such as that derived from FcP_2 coupled with the wealth of experience in the mechanism of directed hydrogenation suggested an alternative approach to the problem. If the hydrogenation is truly heterogeneous, then the mechanism described by Halpern should be general, and neither substrate- nor ligand-specific. On this basis the reactions shown in Figure 28, which exemplify a

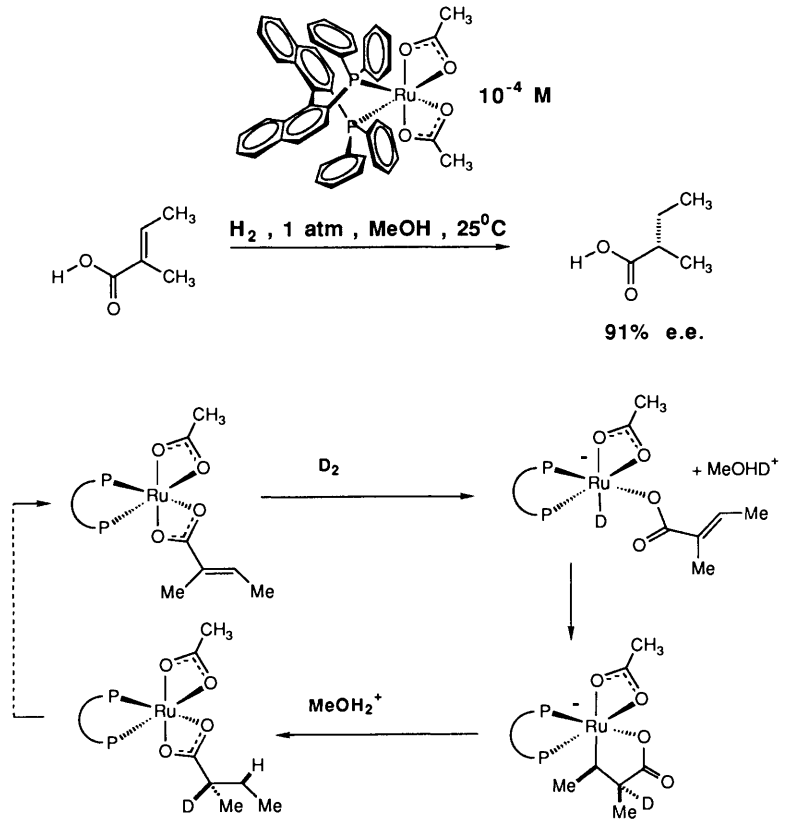

Figure 27 Ashby's and Halpern's mechanism for asymmetric hydrogenation.

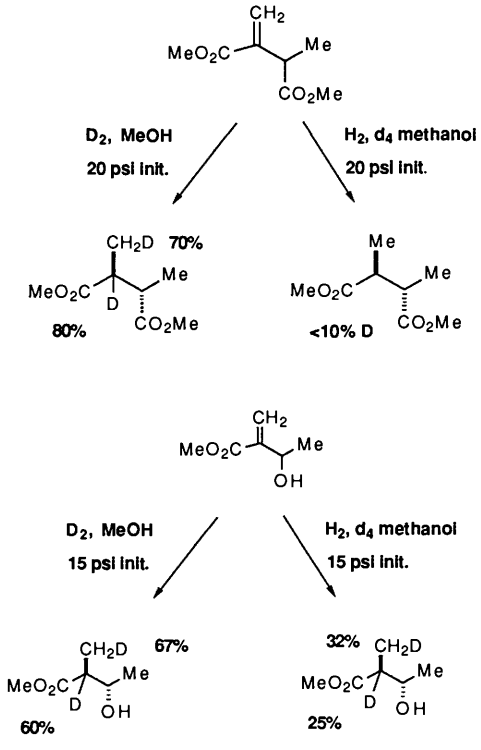

Figure 28 Deuterium distribution in the hydrogenation of racemic chiral substrates with the bis-1,1'-diphenylphosphino (ferrocene) ruthenium complex (Anette Wienand).

wider survey, were carried out.[31] Taking first the diester, previously seen in the context of directed hydrogenation (Section 2), using either the ferrocenyldiphosphine or (±)-BINAP the predominant product with D_2 in MeOH is dideuterated, and the exchanged protium is fairly evenly distributed between the α- and β-carbons. There is very little incorporation of deuterium when the reduction is carried out with H_2 in MeOD. Only with BINAP is the *syn*-diastereomer of product detected and in that case it occurs to the extent of 12%. The stereoselectivity is much lower when the reduction of racemic diester is carried out with the *S*-BINAP Ru complex, since the mismatched catalyst/substrate pair gives close to 1:1 of the two diastereomers of product. In allylic alcohol hydrogenations, *anti*-specificity is again observed with *syn*-product undetected. The isotopic label is much more exchanged when reduction is carried out with D_2 in MeOH; exchange from solvent into product was also readily observed using H_2 in MeOD. But the isotope is again quite evenly distributed between the α- and β-carbons. With (±)-BINAP Ru similar results were obtained although the reduction was much slower.

The results demonstrate that the isotope exchange follows a conventional mechanism and does not require heterolytic activation of molecular hydrogen, with our catalysts at least. The detailed mechanism and the structure of true catalytic intermediates, however, must await further study.

5 Reagent-directed Asymmetric Hydroboration

In most stereoselective catalysis, it is the catalyst itself which is the source of specificity, providing the chiral information leading to asymmetry in the product. In the section on directed hydrogenation, the selectivity arises from internal chirality transfer in the reactant. Since catalysis is normally a three-component reaction (catalyst, reactant, and reagent) a further possibility arises. In an appropriate case the reagent in a catalytic process may contribute to, or even control, the stereochemical course of reaction.

One procedure where a chiral reagent might be used is in rhodium-catalysed hydroboration, normally carried out with catecholborane.[32] Thus initial efforts were directed to the synthesis of simple enantiomerically pure secondary boranes. The oxazaborolidines derived from either hand of ephedrine or ψ-ephedrine proved straightforward to prepare in a two-stage

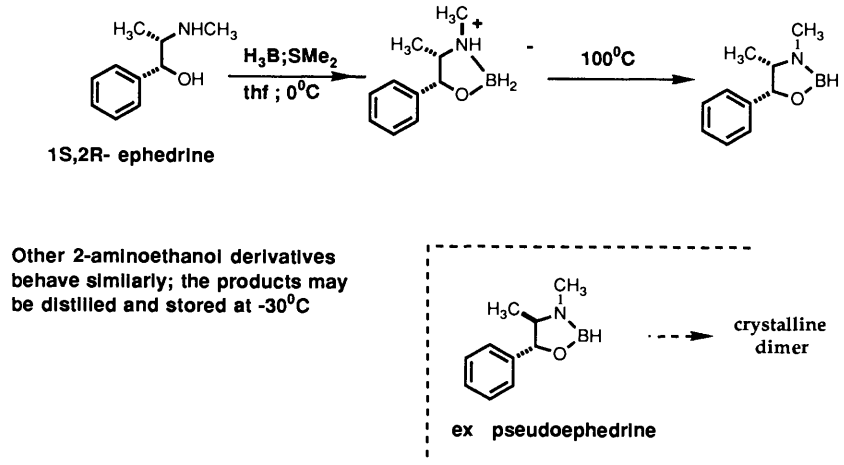

Figure 29 Synthesis of oxazaborolidines (Guy Lloyd-Jones).

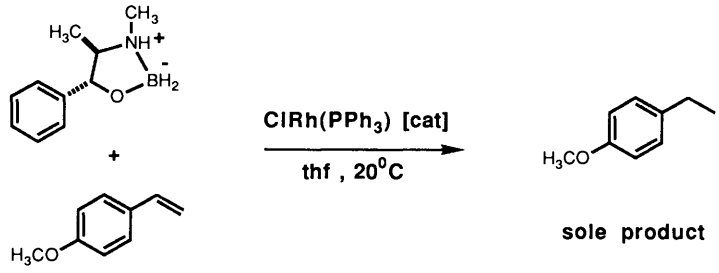

Figure 30 Attempted catalytic hydroboration with the primary borane intermediate. (Guy Lloyd-Jones).

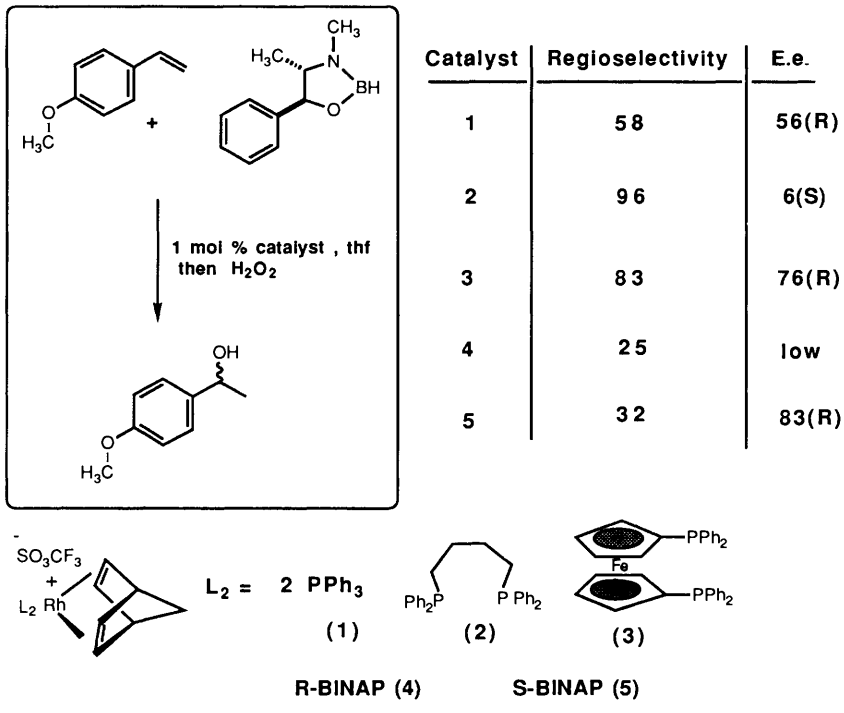

Catalyst	Regioselectivity	E.e.
1	58	56(R)
2	96	6(S)
3	83	76(R)
4	25	low
5	32	83(R)

Figure 31 Catalytic asymmetric hydroboration with the bis-1,1'-diphenylphosphino (ferrocene) rhodium complex and other species (Guy Lloyd-Jones).

procedure as distillable oils. In the latter case the reagent dimerized on standing to a crystalline material whose spectroscopic properties were consistent with a cyclodimeric structure (Figure 29); the dimerization could be reversed by heating in vacuum.[33] The primary borane intermediate was briefly examined as a catalytic hydroboration reagent, but rather functioned as a transfer hydrogenation catalyst (Figure 30).

Through comparative examination of the borane reagents with different Rh catalysts, it was discovered that the highest e.e.s were obtained when ψ-ephedrineborane reacted with *p*-vinylanisole, with FcP_2 as the Rh-bound ligand at ambient temperature. The secondary alcohol isolated after H_2O_2 oxidation had been formed in 76% e.e. and as 83% of total product, the rest being due to regioisomeric alcohol or hydrogenation product (Figure 31). Better regioselectivity could be obtained in

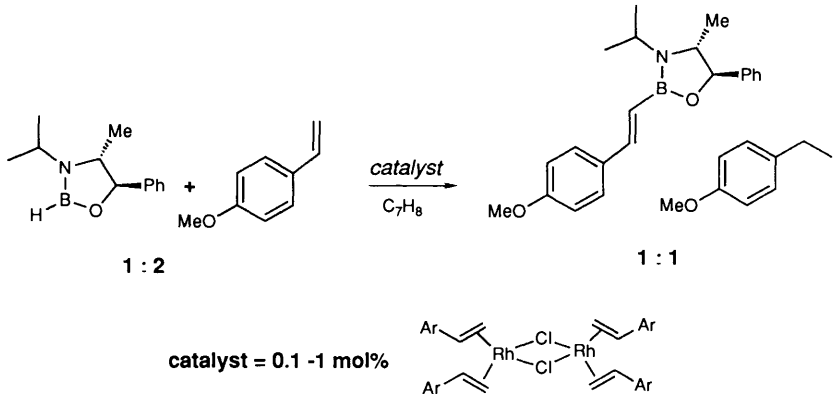

Figure 32 The observation of quantitative disproportionation to vinylborane and hydrogenation product with a bulky secondary borane (Guy Lloyd-Jones).

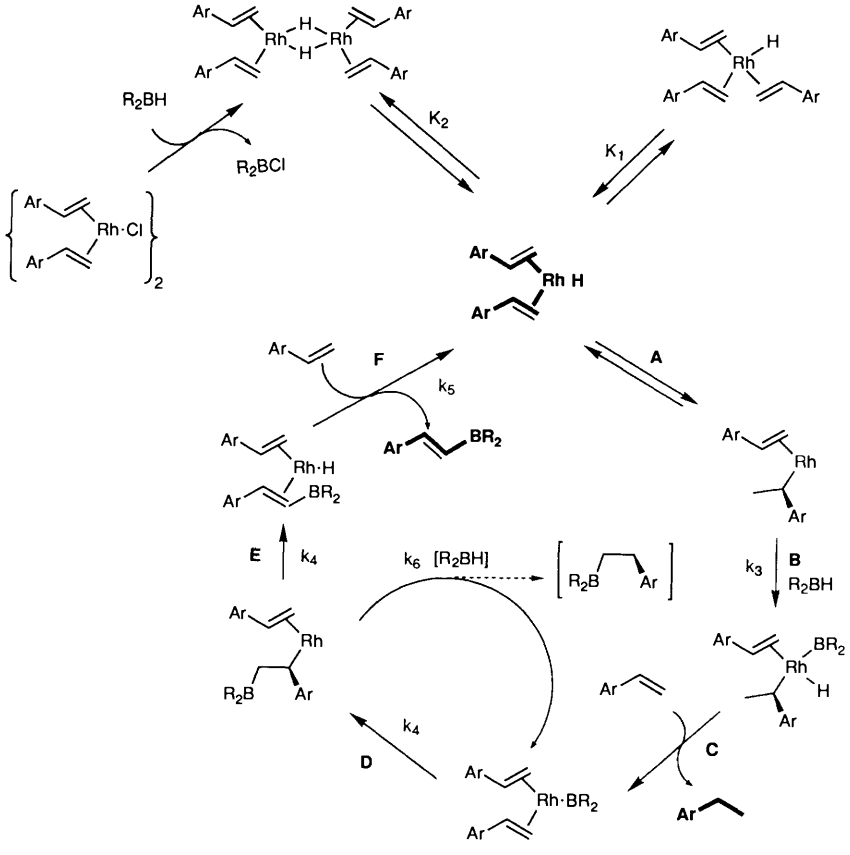

Figure 33 A mechanism for catalytic vinylboration (Guy Lloyd-Jones).

a rapid reaction with the $Ph_2P(CH_2)_4PPh_2$ complex, but there the optical yield was low. With the oxazaborolidine derived from 1*R*,2*R*-ephedrine and *S*-BINAP as ligand, an 85% e.e. was obtained, but the regioselectivity was poor. In contrast, the same reaction with *R*-BINAP-based catalyst occurred very slowly and with low optical yield. This demonstrates that both the catalyst and reagent have a strong influence on the course of the reaction, and will assist in the development of models to assist the understanding and future prediction of enantioselectivity in catalytic hydroboration.

These early results provide an incentive to extend the design of the reagent and hence optimize the enantioselectivity. One factor to be addressed is the role of the substituent on nitrogen in the oxazaborolidine, and whether increasing its steric bulk can enhance the selectivity. For this reason the i-Pr analogue was prepared, and in preliminary experiments shown to react very sluggishly, with hydroboration products only formed at long reaction times. In addition, it appeared that the main products were not derived from simple addition but appeared to result from some addition–elimination process giving rise to hydrogenation and the vinylborane. After further experimentation it was discovered that the reaction did not proceed at all in the complete absence of air; the observed process could be attributed to trace amounts of adventitious oxygen dissipating into the system at long reaction times. NMR observation confirmed that the catalyst had part-decomposed to phosphine oxide under these conditions, which led us to attempt the reaction with a phosphine-free catalyst, the bis(olefin)rhodium chloride dimer.[34] Under these conditions the vinylboration reaction of Figure 32 occurred rapidly and quantitatively.

By a series of experiments with labelled olefin it proved possible to define a mechanism for the reaction consistent with all the facts, with the key intermediate being the rhodium hydride formed in the initial stages. Kinetic studies reveal that

the decay of borane concentration with time varies between the extremes of first- and zero-order, depending on the initial reagent concentrations The results can be accurately simulated with a single set of rate and equilibrium constants according to the mechanism shown Each addition to the styrene is regiospecific, and each step of Figure 33 occurs quantitatively so that the conventional hydroboration pathway (giving secondary borane) is not followed Even with catecholborane, vinylboration is the major pathway under these reaction conditions, although competition from a further addition of borane at the k_6 stage leads to the *primary* borane as a significant product

These results demonstrate the potential complexity of catalytic hydroboration, which needs to be appreciated in the design of superior catalysts and reactants for the asymmetric variant It seems that only rather P-acidic secondary boranes will work effectively with Rh catalysts at least, and the oxazaborolidine approach needs to be modified accordingly This provides one of the many challenges for future work

Acknowledgments The author is deeply grateful to the Royal Society of Chemistry for the award of the Tilden Lecture for 1991 The research described has been carried out by an enthusiastic and highly committed group of postgraduates and postdoctorals who have been a continuing pleasure to work with, their contributions are acknowledged in the Figure captions and references and any credit for the outcome should be directed to them Much of the work has relied on continuing SERC support, augmented by Industry, and on supplies of precious metals on loan from Johnson-Matthey Susan Armstrong and Patrick Guiry made critical comments on the manuscript

6 References

1 L Michaelis and M Menten, *Biochem Z*, 1913, **49**, 333
2 B R James in 'Comprehensive Organometallic Catalysis', Vol 8, ed G Wilkinson, F G A Stone, and E W Abel, Pergamon Press, Oxford, 1982, Chapter 51, pp 285ff
3 M I Page in 'Enzyme Mechanisms', ed M I Page and A Williams, Royal Society of Chemistry, Cambridge, 1987, Chapter 1, p 1
4 N W Alcock, J M Brown, and J J Perez-Torrente, *Tetrahedron Lett*, 1992, **33**, 389
5 J M Brown, P L Evans, and A R Lucy, *J Chem Soc Perkin Trans 2*, 1987, 1589, N Koga and K Morokuma, *Chem Rev*, 1991, **91**, 823, N Koga and K Morokuma, *ACS Symposium Series*, 1989, **394**, 77
6 J Halpern and C R Landis, *J Am Chem Soc*, 1987, **109**, 1746
7 J M Brown, P A Chaloner, and G A Morris, *J Chem Soc Perkin Trans 2* 1987, 1583
8 A S C Chan and J Halpern, *J Am Chem Soc*, 1980, **102**, 838, J M Brown and P A Chaloner, *J Chem Soc Chem Commun*, 1980, 344 J M Brown, L R Canning, A J Downs, and A M Forster, *J Organometallic Chem*, 1983, **255**, 103
9 N W Alcock, J M Brown, A E Derome, and A R Lucy, *J Chem Soc Chem Commun*, 1985, 575, J M Brown and P J Maddox, *J Chem Soc Chem Commun*, 1987, 1276
10 J M Brown and P L Evans, *Tetrahedron*, 1988, **44**, 4905, P L Bogdan, J J Irwin, and B Bosnich, *Organometallics*, 1989, **8**, 1450
11 N W Alcock, J M Brown, and P J Maddox, *J Chem Soc Chem Commun*, 1986, 1532, and references therein, B McCulloch, J Halpern, M R Thompson, and C R Landis, *Organometallics*, 1990, **9**, 1392
12 J M Brown and R G Naik, *J Chem Soc Chem Commun*, 1982, 348
13 J M Brown, *Angew Chem Int Ed Engl*, 1987, **26**, 190, J M Brown, I Cutting, and A P James, *Bull Soc Chim Fr*, 1988, 211, J M Brown, P L Evans, and A P James, *Org Synth*, 1989, **68**, 64, D H Birtwistle, J M Brown, R H Herbert, A P James, K -F Lee, and R J Taylor, *J Chem Soc Chem Commun*, 1989, 194, D Ando, C Bevan, J M Brown, and D W Price, *J Chem Soc Chem Commun*, 1992, 594
14 J M Brown, D I Hulmes, and F I Knight, *J Chem Soc Perkin Trans 2*, 1993, submitted
15 J M Brown and I Cutting, *J Chem Soc Chem Commun*, 1985, 578, J M Brown, I Cutting, P L Evans, and P J Maddox, *Tetrahedron Lett*, 1986, **27**, 3307, J M Brown, A P James, and L M Prior, *Tetrahedron Lett*, 1987, **28**, 2179
16 Some recent references Y D Wu, Y Wang, and K N Houk, *J Org Chem*, 1992, **57**, 1362, M Lautens and P H M Delanghe, *J Org Chem*, 1992, **57**, 798, D A Evans and S A Kaldor, *J Org Chem*, 1990, **55**, 1698
17 J M Brown and P J Maddox, *J Chem Soc Chem Commun*, 1987, 1276, J M Brown and P J Maddox, *Chirality*, 1991, **3**, 345
18 N W Alcock, J M Brown, A D Conn, A P James, and R J Taylor, to be published
19 J M Brown and D W Price, to be published
20 D Parker, *Chem Rev*, 1991, **91**, 1441
21 R J McKinney and F J Weigert, Quantum Chemistry Program Exchange, Program QCMP022, 1987
22 H Brunner and W Leitner, *Angew Chem Int Ed Engl*, 1988, **27**, 1180, H Brunner, E Graf, W Leitner, and K Wutz, *Synthesis*, 1989, 743
23 G W Kirby and A Michael, *J Chem Soc Perkin Trans 1*, 1973, 115
24 J M Brown, A E Derome, G D Hughes, and P K Monaghan, *Aust J Chem*, 1992, **45**, 143
25 W Leitner, J M Brown, and H Brunner, *J Am Chem Soc*, 1993, **115**, in press
26 R Noyori, M Ohta, Y Hsiao, M Kitamura, T Ohta, and H Takaya, *J Am Chem Soc*, 1986, **108**, 7117, H Takaya, T Ohta, N Sayo, H Kumobayashi, S Akutagawa, S Inoue, I Kasahira, and R Noyori, *J Am Chem Soc*, 1987, **109**, 1596 and later papers, R Noyori and M Kitamura, *Modern Synthetic Methods*, 1989, **6**, 131
27 R R Schrock, B F G Johnson, and J Lewis, *J Chem Soc Dalton Trans*, 1974, 951
28 N W Alcock, J M Brown, M Rose, and A Wienand, *Tetrahedron Asymmetry*, 1991, **2**, 47
29 J M Brown, H Brunner, W Leitner, and M Rose, *Tetrahedron Asymmetry*, 1991, **2**, 331
30 M T Ashby and J Halpern, *J Am Chem Soc*, 1991, **113**, 589, T Ohta, H Takaya, and R Noyori, *Tetrahedron Lett*, 1990, **31**, 7189
31 J M Brown and A Wienand, to be published
32 K Burgess and M J Ohlmeyer, *Chem Rev*, 1991, **91**, 1179
33 J M Brown and G C Lloyd-Jones, *Tetrahedron Asymmetry*, 1990, **1**, 869
34 J M Brown and G C Lloyd-Jones, *J Chem Soc Chem Commun*, 1992, 710